

This is the accepted manuscript made available via CHORUS. The article has been published as:

## Fixed-node diffusion Monte Carlo description of nitrogen defects in zinc oxide

Jaehyung Yu, Lucas K. Wagner, and Elif Ertekin

Phys. Rev. B **95**, 075209 — Published 27 February 2017

DOI: [10.1103/PhysRevB.95.075209](https://doi.org/10.1103/PhysRevB.95.075209)

# Fixed node diffusion Monte Carlo description of nitrogen defects in zinc oxide

Jaehyung Yu<sup>1</sup>, Lucas K. Wagner<sup>2</sup>, and Elif Ertekin<sup>1,3</sup>

<sup>1</sup>*Department of Mechanical Science & Engineering, 1206 W Green Street,  
University of Illinois at Urbana-Champaign, Urbana IL 61801*

<sup>2</sup>*Department of Physics, University of Illinois at Urbana-Champaign, Urbana IL 61801 and*

<sup>3</sup>*International Institute for Carbon Neutral Energy Research (WPI-I<sup>2</sup>CNER),  
Kyushu University, 744 Moto-oka, Nishi-ku, Fukuoka 819-0395, Japan\**

Using fixed-node diffusion Monte Carlo (FN-DMC), we evaluate the formation energies and charge transition levels of substitutional nitrogen defects in the wide band gap semiconductor zinc oxide. The use of a direct-solution, many-body approach inherently secures a good description of electron-electron interactions, achieving high accuracy without adjustable parameters. According to FN-DMC nitrogen is a deep acceptor with a charge transition level 1.0(3) eV above the valence band maximum when 72 atom supercells are used. This result falls on the lower end of typically reported hybrid density functional results for the same sized supercells, which range from 1.0 - 1.8 eV. Further, residual finite size effects due to charged defect image interactions in the 72 atom supercells are estimated by supercell extrapolation within hybrid density functional theory. When the finite size correction is included, we obtain a deep acceptor at 1.6(3) eV. This result is in good agreement with recent experimental measurements. We also analyze the local compressibility of charge according to FN-DMC and common density functionals, and find that the use of hybrid functionals obtain compressibilities in better agreement with the many-body theory. Our work illustrates the application of the FN-DMC method to a challenging point defect problem, demonstrating that uncertainties and approximations can be well-controlled.

## I. INTRODUCTION

The introduction of point defects dramatically changes the properties of semiconducting materials, even in small concentrations<sup>1,2</sup>. Characterizing how point defects affect semiconductor properties is critical to designing materials for electronic, optical, and optoelectronic devices. Historically, first-principles descriptions of the properties of point defects in semiconductors has been challenging<sup>1,2</sup>. Density functional theory<sup>3,4</sup> (DFT) remains the most widely used method for this purpose. In spite of recent advances such as the use of hybrid DFT<sup>5</sup>, GW<sup>6</sup>, and a generalized Koopman's method<sup>7</sup>, questions to the quantitative accuracy attainable still remain, and often similar defect calculations can result in different predictions. The challenges broadly arise from two sources: errors inherent to DFT's approximate treatment of electron-electron interactions, and finite size effects from practical limitations to the computational domain.

Substitutional nitrogen ( $N_O$ ) in zinc oxide is a classic example of a challenging point defect to describe theoretically. Nitrogen had long been considered the most likely candidate for achieving  $p$ -type conductivity in this wide band gap semiconductor. Early experiments suggested nitrogen to be a shallow acceptor with a charge transition level (CTL)  $\epsilon(0/-)$  close to the valence band edge<sup>8</sup>. Meanwhile early computational results based on conventional density functional methods (LDA, GGA) predicted the charge transition level to occur at  $\epsilon(0/-) \approx 0.4$  eV above the valence band edge<sup>9</sup>. However, subsequent reproducibility of the experiments has proven to be challenging, and more recent computational results based on hybrid functional DFT<sup>10,11</sup>, a generalized Koopman's

framework<sup>12</sup>, and a comprehensive DFT study using different exchange-correlation functionals<sup>13</sup> suggest instead a deep nature but with  $\epsilon(0/-)$  reported in a wide range 1.0 - 2.1 eV above the VBM. Recent experiments based on photoluminescence spectroscopy find the N acceptor level to lie 1.4 eV above the VBM<sup>2,14,15</sup>.

Quantum Monte Carlo (QMC)<sup>16,17</sup>, specifically the fixed-node diffusion Monte Carlo (FN-DMC) flavor<sup>18-20</sup>, is one of the newer first-principles approaches for the prediction of defect properties of semiconductors<sup>21,22</sup>. In QMC, stochastic sampling is used in the solution of the interacting many-body Schrödinger equation. Due to their direct treatment of electron correlation, QMC methods inherently secure an accurate description of many-body interactions among electrons. QMC obtains high accuracy for ground state and excited state properties<sup>21-24</sup>, at the cost of higher computational effort and many-body finite size effects that must be converged.<sup>25,26</sup> FN-DMC defect property simulations of CTLs have been carried out on  $F$ -center defects in MgO<sup>21</sup> and oxygen vacancies in zinc oxide<sup>22</sup>, and show promising results.

In this work, we carry out FN-DMC calculations of  $N_O$  in ZnO and demonstrate that reference values from QMC can be obtained for this system with all errors controlled. We further observe how the FN-DMC description of the defect state compares to other commonly applied techniques such as convention and hybrid exchange DFT. We assess the effect of symmetry breaking distortions of the defect geometry on supercell total energies within DMC, and find that they are comparable to hybrid functional descriptions. For 72 atom supercells, we obtain a CTL of  $\epsilon(0/-) = 1.0(3)$  eV, in reasonable agreement with but on the lower end of other sophisticated

TABLE I. Typical sources of uncertainties in first-principles defect calculations. The first two arise from the approximations inherent to density functional theory and are largely addressed by FN-DMC. The next three arise from finite size effects due to computational limitations on the supercell size. The final item is specific to neutral  $N_O$  in ZnO: the geometry of the neutral defect varies for different descriptions of exchange/correlation in DFT.

Potential source of error	Underlying reason	Correction approach
chemical potentials $\mu_i$	approximate treatment of electron-electron interactions	improved by FN-DMC
band gap	approximate treatment of electron-electron interactions	improved by FN-DMC
elastic finite size effect	finite supercell size	use large supercell; estimate remaining interaction
ionized supercell interaction & potential alignment	finite supercell size	use large supercell; estimate remaining interaction
Burstein-Moss type effect	finite supercell size	N/A for deep defects
geometry of neutral defect?	DFT - geometry depends on exchange correlation functional	assess candidate geometries in FN-DMC

first-principles results. As an estimate of the remaining charged defect image interactions in the 72 atom supercells, we carry out supercell extrapolations within DFT-PBE0 and find that the CTL further deepens to 1.6(3) eV. Further, we compare the local compressibility of charge according to DMC, DFT-PBE, and DFT-PBE0, which clearly demonstrates the bias of conventional density functional theory towards delocalized, shallow defect states. This work highlights the potential advantages and challenges in the application of QMC approaches to the calculation of point defect properties.

## II. METHODS

Defect formation energies (DFEs) are obtained according to the usual formalism<sup>27</sup>

$$\Delta E(N_O^q) = (E(N_O^q) - E_{perf}) + (\mu_O - \mu_N) + q(\epsilon_F + \epsilon_V). \quad (1)$$

Here,  $E(N_O^q)$  is the total energy of a supercell containing a defect  $N_O^q$  in the charge state  $q = (0, -1)$  and  $E_{perf}$  is total energy of the corresponding perfect supercell.  $\mu_i$  is the chemical potential of atomic species  $i$ , which describes the thermodynamic environment under which the defect forms; we report DFEs under the Zn-rich limit. The Fermi level of semiconductor  $\epsilon_F$  varies from  $0 < \epsilon_F < E_g$  where  $E_g$  is band gap, and is referenced to the valence band maximum  $\epsilon_V$ . The CTL  $\epsilon(0/-)$  is given by the value of  $\epsilon_F$  for which  $\Delta E(N_O^0) = \Delta E(N_O^{-1})$ .

Prior to carrying out FN-DMC defect calculations, we considered the typical sources of uncertainty that arise when evaluating DFEs from Eq. (1) in DFT. These are arranged according to the underlying reason for the uncertainty – either the treatment of exchange/correlation or finite size effects – in Table I. The approximate treatment of electron-electron interactions can give rise to uncertainties which can manifest as problems with (i) the range of chemical potentials  $\mu_i$ , since the computed formation enthalpies of the semiconductor and/or parent compounds (*i.e.*, ZnO,  $O_2$ , and  $N_2$  for us) are not per-

fect, and (ii) well-known band gap problems. The use of periodic boundary conditions with finite sized supercells induce spurious interaction between the defect and its images. The (iii) largely elastic effects are typically more short-ranged, but (iv) for  $q \neq 0$ , electrostatic interactions between charged defects are long-ranged. Also, (v) for shallow defects finite-sized supercells can artificially induce a Burstein-Moss type<sup>1,28</sup> band-filling effect. Finally, for  $N_O$  in ZnO, there is a question of the geometry of the neutral defect, as the relaxed configuration shows a sensitivity to selected DFT functional<sup>12,29</sup>. Our approach to addressing each of these is described later.

Our FN-DMC calculations are carried out using the QWalk<sup>30</sup> code. We use spin-polarized, single-determinant Slater-Jastrow trial wave functions constructed from DFT-PBE0 Kohn-Sham orbitals, with variance-minimized two-body Jastrow coefficients, and a time step of 0.004 a.u. Time step errors are converged to within 0.02 eV/f.u.<sup>24</sup>. The orbitals are obtained from spin-polarized DFT-PBE0 simulations using CRYSTAL14<sup>31</sup>, and are expanded in a Gaussian-type localized basis set. We use Trail-Needs pseudopotentials<sup>32,33</sup>; for Zn this leaves the  $4s^2 3d^{10}$  electrons in valence. The T-moves scheme<sup>34</sup> is used to reduce pseudopotential localization errors. Twist-averaged boundary conditions corresponding to an effective  $2 \times 2 \times 2$   $k$ -grid are used to calculate supercell total energies. We use a 72 atom ZnO supercell ( $3 \times 3 \times 2$  supercell of the 4 atom wurtzite unit cell) with experimental lattice constants for calculating DFEs. Due to challenges with geometry optimization in QMC, we use DFT relaxed geometries, also discussed later.

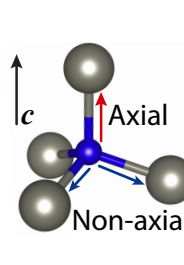
Our previous work<sup>24</sup> showed that when this simulation protocol is adopted, we obtain atomization energies for ZnO solid,  $O_2$ , and  $N_2$  within 0.05 eV/f.u. The calculated optical excitation is 3.8(2) eV, and probably overestimates the experimental value of 3.4 eV (compare: DFT-PBE, DFT-HSE06, and DFT-PBE0 gaps of 0.7 eV, 2.4 eV, and 3.3 eV respectively). Thus, the first two sources of uncertainty in Table I are largely inherently addressed in FN-DMC and we choose to live with any remaining un-

certainty. We emphasize that these results are obtained with no adjustable parameters.

To address finite size effects, we use as large a supercell as feasible in FN-DMC (72 atoms) and estimate the remaining finite size corrections by supercell extrapolation. Due to the computational restrictions of FN-DMC, our extrapolations are always carried out using DFT-PBE0, which is expected to give the most realistic description of the dielectric constant, necessary to obtain a good estimate of screening and the charged defect interaction. Furthermore, the corresponding estimates of the finite size effects are included as corrections to the 72 atom supercell FN-DMC results. Ideally the extrapolation would also be carried out in FN-DMC but this is not computationally tractable. Although 72 atom supercells are small, they are not much smaller than accessible for typical hybrid DFT supercell calculations. We confirmed by extrapolating to larger supercells in DFT-PBE0 that for neutral  $N_O$ , supercell total energies are converged to within 0.03 eV, indicating that the elastic finite size effects are under control (not shown). Thus, the items in Table I that remain to be addressed are the charged supercell interactions and the question of defect geometry.

### III. RESULTS AND DISCUSSION

We present our results in terms of the quantities in Eq. (1) that must be evaluated to obtain the DFEs and CTLs. As this is a first attempt to apply FN-DMC to such a complex defect problem, we report all our computed values here so that others may reproduce our results. Often previous reported results for 72 atom supercells do not include a direct estimate of the charged defect image interaction, so we first present our results for 72 atom supercells without interaction as well. This allows direct comparison of ours to other corresponding predictions. We later discuss the incorporation of the finite size effect and how it modifies our predicted value.



	Distorted	Symmetric
Axial (Å)	2.077	1.951
Non-axial (Å)	1.951	1.945
$\Delta E_{rel}^{PBE0}$ (eV)	-0.17	0
$\Delta E_{rel}^{DMC}$ (eV)	$-0.12 \pm 0.33$	0

FIG. 1. Bond length between neutral N (blue) and Zn (grey) in supercell.  $\Delta E_{rel}$  refers relative total energy of FN-DMC between 2 given neutral geometry.

#### A. Supercells with Neutral and Charged Defects

Supercells containing 72 atoms are used in FN-DMC to sample configurations and directly obtain the quantities  $E(N_O^0)$  and  $E(N_O^{-1})$ . This is straightforward for  $E(N_O^{-1})$  since different DFTs predict similar relaxed geometries. However for  $N_O^0$  there is a possibility of symmetry-breaking distortions (polaron formation) that stabilize the neutral defect and deepen the CTL. Standard DFT calculations based on PBE obtain only small, symmetric relaxations of atoms around  $N_O^0$ . On the other hand, hybrid calculations for suitably large supercells find a symmetry broken configuration to be more favorable<sup>12,13</sup>, and EPR measurements are also consistent with the presence of a distorted, deep state<sup>29</sup>. The distorted state corresponds to an asymmetric elongation along the  $c$  direction N–Zn bond shown in Fig. 1. In the distorted configuration the N  $2p$  orbitals are split into planar  $2p_{x,y}$  and  $2p_z$  orbitals. We assessed this within the CRYSTAL14 code, and also find that in PBE  $N_O^0$  defect always relaxes back to a symmetric configuration. Within PBE0 we also observe metastable symmetric and asymmetric configurations of  $N_O^0$ , with distortions as summarized in Fig. 1.

Since geometry relaxations in FN-DMC are currently not tractable for large systems, we selected both as candidate configurations for  $N_O^0$  and compared their energies  $E(N_O^0)_{asym}$  and  $E(N_O^0)_{sym}$  directly in FN-DMC. According to FN-DMC the distorted state is  $0.12 \pm 0.33$  eV lower in energy than the symmetric configuration, a good match to the PBE0 value which is 0.17 eV, see Table II. The computational cost makes it difficult for us to better resolve the energy difference, but the results suggest that the symmetry-breaking distortion cannot solely be responsible for the deep nature of the defect<sup>35</sup>.

#### B. Chemical Potentials

DFEs are reported in the Zn-rich, O-poor limit. The chemical potential difference in Eq. (1),  $\mu_O - \mu_N$ , is thus given by  $\frac{1}{2}\mu_{O_2} - \frac{1}{2}\mu_{N_2} - \Delta H_{ZnO}$  where  $\Delta H_{ZnO}$  is the formation enthalpy of ZnO, equal to 3.606 eV under standard conditions.  $\mu_{O_2}$ ,  $\mu_{N_2}$  are the energies of the molecules under standard conditions, obtained by adding a thermodynamic correction<sup>36</sup> for pressure/volume and temperature/entropy contributions to the total energies obtained from DMC calculations (corresponding to  $T = 0$  K,  $P = 0$ ). The quantity  $\mu_O - \mu_N$  affects the absolute value of the DFEs for the neutral and charged defect, but not the CTL.

#### C. Valence band maximum

The next term in Eq. (1) that needs to be addressed is  $\epsilon_V$ , the position of the VBM. In DFT the Kohn-Sham eigenvalues are arbitrary to within a constant that is

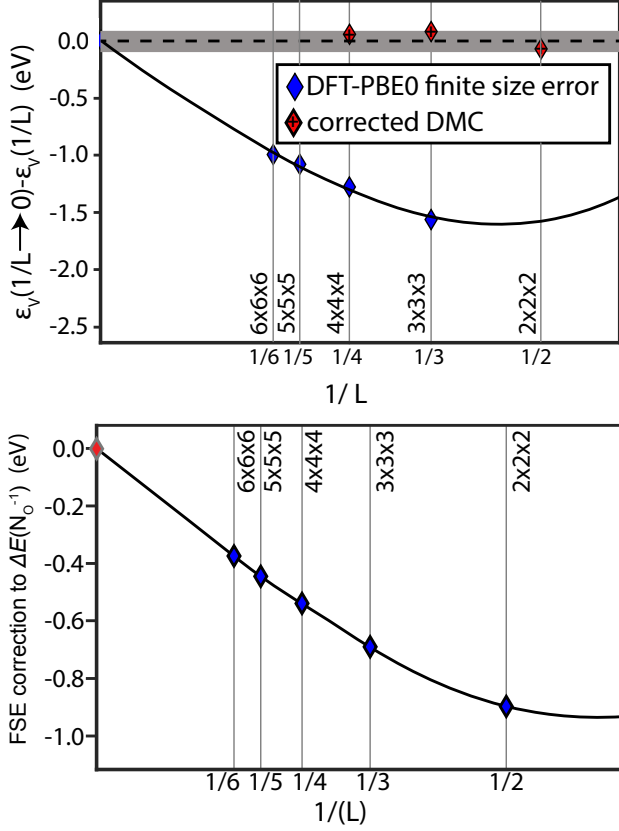


FIG. 2. Supercell extrapolations carried out with DFT-PBE0 that show the finite size effect (FSE) corrections for (a) the ionization potential and (b) electrostatic image interactions between ionized nitrogen defects. The x-axis indicates  $1/L$ , where  $L \times L \times L$  is the number of unit cells in the supercell. The y-axis is the FSE correction for a given supercell; in the limit of an infinite sized supercell, the FSE corrections go to zero. In (a) the DMC values with the finite size correction applied are within statistical error (0.1 eV).

determined by the average electrostatic potential in the simulation supercell. This average electrostatic potential itself depends on how the Ewald summations are carried out within the code. To use Eq. (1), the value of  $\epsilon_V$  must be determined with respect to the same average electrostatic potential as the pure host semiconductor (ZnO).

The situation is more complicated in QMC, since  $\epsilon_V$  is a single-particle property that rigorously does not exist in true many-body descriptions. The corresponding quantity is instead the ZnO ionization potential  $IP = E_0 - E_+$ , the energy cost to remove an electron from the system.  $E_0$  is the energy of neutral ZnO, and  $E_+$  is the energy of ZnO with one hole (thus, positively charged). This expression should be evaluated in the thermodynamic limit of infinite sized supercells, but supercells larger than 72 atoms are computationally prohibitive in FN-DMC for the resources currently available to us. Therefore our approach is to evaluate the IP using 72 atom supercells in FN-DMC, and then carry out supercell extrapolations in DFT-PBE0 to estimate the

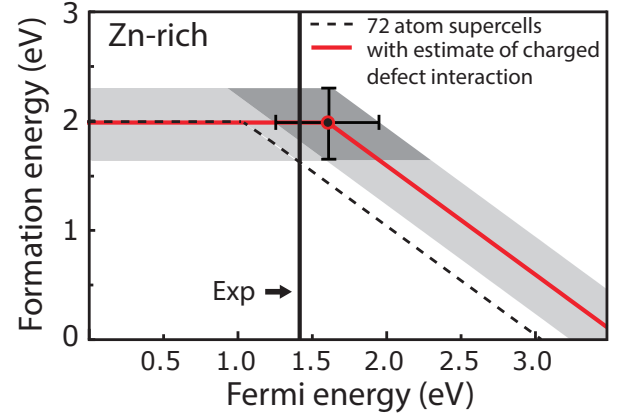


FIG. 3. Defect formation energies and charge transition levels for nitrogen in zinc oxide. Experimental ionization level<sup>15</sup> is shown as black solid line. The gray lines indicate stochastic error bars around the computed quantities.

finite size correction to this cell. To simplify the extrapolation, we used the zinc blende structure of ZnO which allows us to use uniform supercells; since they have similar electronic structure and dielectric constants we assume the trends are comparable.

Our DFT-PBE0 extrapolation is shown in Fig. 2a in blue, where fitted curve includes terms to first and third order in  $1/L$ . In the limit, this extrapolates to the  $IP$  with respect to the average electrostatic potential in the supercell, rather than an absolute reference. For the smaller supercells we evaluated the IP within DMC as well, and find that the trends (within error bars) are consistent. The PBE0 trends in Fig. 2a are used to estimate the correction to the  $IP$  obtained in the 72 atom supercell in FN-DMC. We also show with the dashed line the DMC results with the finite size correction applied. The corrected values are shown to be equivalent within an uncertainty of 0.1 eV. Thus the uncertainty in our calculated ionization potential is estimated to be around 0.1 eV.

#### D. Charge transition levels and discussion

The DFEs  $\Delta E(N_O^0)$  and  $\Delta E(N_O^{-1})$  computed within 72 atom supercells from Eq. (1) as described above are summarized in Table II, and plotted with the dashed, black line in Fig. 3. The corresponding CTL is  $\epsilon(0/-) = 1.0(3)$  eV. This value can be directly compared to the value of 1.3 eV obtained in Ref. [10] using the HSE hybrid functional and the value of 1.6 eV obtained in Ref. [12] obtained with the generalized Koopman's formalism, for the same sized system. The CTLs according to Ref. [13] obtained within PBE0 are reported as 1.1-1.2 eV from 72 atom supercells, but include an  $\approx 0.2$  eV estimate of the charged defect image interaction, so the direct comparison is 0.9-1.1 eV<sup>37</sup>. Likewise, the CTLs according to Ref. [11] are reported as 2.1 eV for 72 atom supercells,



TABLE II. Defect formation energies for neutral and negatively ionized nitrogen defects for 72 atom supercells according to FN-DMC. Results are reported for Zn-rich conditions, with the Fermi level at the VBM. For neutral defect, both the symmetric and the distorted configurations are shown. The last row gives the finite size correction to the 72 atom supercell estimated from DFT(PBE0).

Quantity	eV
$\Delta E(N_O^0)(N_a = 72)$ , distorted	1.9(0.2)
$\Delta E(N_O^0)(N_a = 72)$ , symmetric	2.0(0.2)
$\Delta E(N_O^{-1})(N_a = 72)$	3.0(0.2)
$\Delta E(N_O^{-1})(N_a = \infty) - \Delta E(N_O^{-1})(N_a = 72)$ (estimated from DFT-PBE0)	0.6

but include an  $\approx 0.3$  eV estimate of the charged defect image interaction, so the direct comparison is 1.8 eV. Although the different simulation protocols make direct comparisons difficult, it appears that FN-DMC value of the CTL lies on the lower end of the range of values reported in hybrid DFT calculations (0.9-1.8 eV). This suggests that, at least for this particular defect problem, hybrid functional DFT may exhibit a tendency towards over-localization of the defect states and, relatedly, a too deep prediction of the CTL.

Possible sources of uncertainty within FN-DMC should also be considered. Our previous work<sup>24</sup> suggests that the largest sources of uncertainty may come from residual many-body finite size effects inherent to DMC and other many-body theories (different from the supercell finite size effect for defect simulations). Based on our previous experiences with zinc oxide<sup>24</sup>, we estimate that these uncertainties are  $< 0.05$  eV/f.u. Other sources of uncertainty that may be present arise from the fixed node approximation, and our estimate of DFEs rely on a cancellation of nodal errors in the pristine *vs.* defect-containing supercell. Although it is not possible to know the extent of nodal effects, our previous work in FN-DMC simulations of bulk ZnO suggests that the dependence of DMC energies on the DFT functional used to generate the trial wave function is small,  $< 0.05$  eV/f.u.

### E. Estimate of Charged Defect Interactions

Supercells with  $N_O^{-1}$  suffer from long-ranged Coulomb interactions that introduce an (artificial) stabilizing effect on the quantity  $E(N_O^{-1})$  in Eq. (1). To account for the interactions, it is possible to obtain  $E(N_O^{-1})$  for supercells of varying size, and extrapolate to the thermodynamic limit. An approximate form for the extrapolation is given by

$$E_T\left(\frac{1}{L}\right) = E_T\left(\frac{1}{L} \rightarrow 0\right) - \frac{A}{L} - \frac{B}{L^3}, \quad (2)$$

where  $L$  is the supercell side length for a cubic cell, and  $A, B$  are fitting parameters. The first term corresponds to a Madelung contribution and the second to the inter-

action of the localized defect charge distribution with the uniform compensating background<sup>38-40</sup>.

We again carried out the extrapolation in DFT-PBE0 to supercells containing as many as 432 atoms and used this to estimate the correction to our FN-DMC results. The extrapolation is shown in Fig. 2b. The correction to  $E(N_O^{-1})$  for our 72 atom supercells to the thermodynamic limit is around +0.6 eV, as indicated in Table II. The 0.6 eV correction is large, but not atypical of other extrapolated estimates of charged defect interactions in other semiconductors and/or insulators for supercells of this size<sup>39,40</sup>. This correction to  $E(N_O^{-1})$  deepens  $\epsilon(0/-)$  by the same amount. When it is included, our estimated CTL is  $\epsilon(0/-) = 1.6(3)$  eV. This is shown in Figure 3 by the red line. Thus, without accounting for the charged defect finite size effect, our CTL is 1.0(3) eV, but with our estimated of the finite size effect it becomes 1.6(3) eV. These two results can be compared to recent experimental measurements from photoluminescence, which report the level as 1.4 eV<sup>15</sup>.

Although the prediction of a CTL of 1.6(3) eV appears on the surface to be in good agreement with several recent results, such as a hybrid functional value of 1.4 eV<sup>10</sup> and the value of 1.6 eV obtained in a generalized Koopman's approach<sup>12</sup>, we note that the manner in which we obtain our value is slightly different. All of these quoted values are obtained for 72 atom supercells, but for consistency should be compared to our DMC value of 1.0(3) eV obtained without the charged defect interaction estimate. Thus, it appears that for this particular defect problem, DMC probably finds the CTL to be somewhat less deep. We caution against assuming this tendency to be true in general however. This is first due to our error bars. Second, it may be the case that the performance of hybrid functionals, rather than exhibiting systematic biases, may be more material specific. For instance, by contrast for the problem of the aluminum impurity in  $\alpha$ -quartz, the standard hybrid functional description appears still too delocalized<sup>41</sup>.

### F. Local compressibility.

In order to obtain some insights into the differences arising from different theories, we calculated the local compressibility of charge, also known as the site-resolved charge fluctuations. The local compressibility is the expectation value  $\langle \Psi | (\hat{n}_i - \langle \hat{n}_i \rangle)^2 | \Psi \rangle$ , where  $n_i$  is the number operator on the Voronoi polyhedron surrounding atomic site  $i$ . It indicates the degree of localization: if the local compressibility is large, charges on that site are more mobile and delocalized. In Fig. 4 we compare the compressibility for Zn, O, and  $N_O^0$  atoms for FN-DMC, DFT-PBE, and DFT-PBE0, resolved separately for spin up and spin down electrons. For DFT-PBE and DFT-PBE0, the compressibility is obtained by constructing a Slater determinant using the DFT orbitals and evaluating the expectation value as described above.

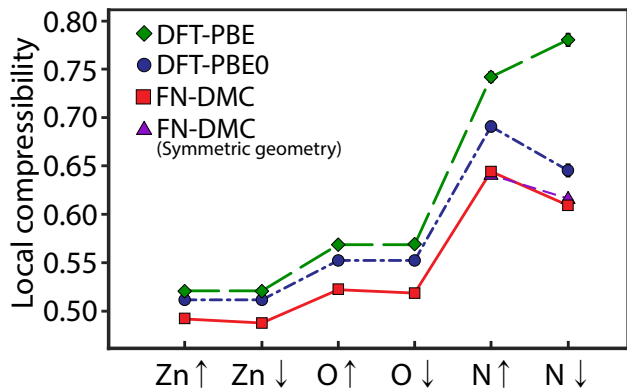


FIG. 4. Charge fluctuations of each spin on the site of Zn, O, and N atoms in the 72 atom supercell. Stochastic uncertainties are smaller than the symbols.  $\uparrow$  denotes the majority and  $\downarrow$  the minority spin.

As shown in Fig. 4, the trends in the compressibility across the different sites and spins are qualitatively similar to each other, with the fluctuations smallest on the Zn atoms, and largest on the N atom site. However, the compressibilities are too large in DFT-PBE across the board, reflecting the over-hybridization and the overly delocalized description, compared to FN-DMC. DFT-PBE0 brings the values into better agreement with the FN-DMC results. This is consistent with our previous observations for solid MgO<sup>42</sup> and MnO<sup>23</sup>. Interestingly, both DFT-PBE and DFT-PBE0 track the changes in the compressibility across different sites qualitatively correctly for the Zn and the O atoms. One surprising feature is the charge fluctuations of DFT-PBE at the nitrogen atom site. In our notation,  $\uparrow$  denotes the majority spin and  $\downarrow$  the minority spin (these only differ at the defect site, since N has an odd number of electrons). Here, the discrepancy between the DFT-PBE and the FN-DMC results becomes larger and also there is a qualitative failure of DFT-PBE to track the fluctuations correctly. It predicts larger fluctuations in the minority spin, in contrast to FN-DMC. This again is consistent with an over-hybridization and too delocalized description of the N  $2p$  orbitals. Remarkably, DFT-PBE0 recovers the correct ordering and brings the fluctuations at the N site into better agreement with FN-DMC.

Lastly, we wanted to determine if the local compressibility obtained in FN-DMC exhibits sensitivity to the trial wave function and to whether there is a distortion present in the neutral defect geometry. The compressibility for the symmetric configuration of the defect (purple

dash line) as predicted by FN-DMC with DFT-PBE trial wave functions is also shown in Fig. 4. It is found to lie within error bars of the result for the distorted geometry with DFT-PBE0 trial wave functions. The insensitivity of FN-DMC to the trial wave function for pure ZnO was also observed in our previous work<sup>24</sup>. It thus appears that this qualitative description is the same regardless of the DMC trial function or the geometry of the defect.

#### IV. CONCLUSIONS

In conclusion, we assessed the defect formation energies and charge transition levels for substitutional nitrogen in ZnO using fixed-node diffusion Monte Carlo. We find that the nitrogen acceptor level is located 1.0(3) eV above the VBM for 72 atom supercells. This value is obtained using a systematically improvable, parameter free many-body approach. Our computed charge transition level appears to fall in the lower range of values typically reported in hybrid density functional theory results. Superposing a DFT-PBE0 estimate of the finite size effect due to charged defect interactions, the acceptor level is further deepened to approximately 1.6(3) eV. Our work illustrates the application of the FN-DMC method to a challenging point defect problem, demonstrating that uncertainties and approximations can be well controlled. Regarding the use of DFT for defect calculations, analysis of local compressibilities suggest that the use of hybrid functionals can improve the description of defect charge transition levels, providing results in better agreement with the many-body theory.

#### ACKNOWLEDGMENTS

We acknowledge financial support to J. Yu through the Computational Science and Engineering Fellowship Program at the University of Illinois. L.K.W. was supported by the U.S. Department of Energy, Office of Science, Office of Advanced Scientific Computing Research, Scientific Discovery through Advanced Computing (SciDAC) program under Award Number FG02-12ER46875. This research is part of the Blue Waters sustained petascale computing project, which is supported by the National Science Foundation (award No. OCI 07-25070 and ACI-1238993) and the state of Illinois. Blue Waters is a joint effort of the University of Illinois at Urbana-Champaign and its National Center for Supercomputing Applications. Also, this research used resources of the Argonne Leadership Computing Facility, which is a DOE Office of Science User Facility supported under Contract DE-AC02-06CH11357.

\* e-mail: ertekin@illinois.edu

<sup>1</sup> C. Freysoldt, B. Grabowski, T. Hickel, J. Neugebauer, G. Kresse, A. Janotti, and C. G. Van de Walle, [Reviews](#)

- of Modern Physics **86**, 253 (2014).
- <sup>2</sup> A. Alkauskas, M. D. McCluskey, and C. G. Van de Walle, *Journal of Applied Physics* **119**, 181101 (2016).
  - <sup>3</sup> P. Hohenberg and W. Kohn, *Phys. Rev.* **136**, B864 (1964).
  - <sup>4</sup> W. Kohn and L. J. Sham, *Physical Review* **140** (1965), 10.1103/PhysRev.140.A1133.
  - <sup>5</sup> J. Heyd, G. E. Scuseria, and M. Ernzerhof, *Journal of Chemical Physics* **118**, 8207 (2003).
  - <sup>6</sup> L. Hedin, *Physical Review* **139**, A796 (1965).
  - <sup>7</sup> S. Lany and A. Zunger, *Physical Review B - Condensed Matter and Materials Physics* **80**, 1 (2009), arXiv:0905.0018.
  - <sup>8</sup> M. Joseph, H. Tabata, and T. Kawai, *Japanese Journal of Applied Physics* **38**, 1205 (2000).
  - <sup>9</sup> C. H. Park, S. B. Zhang, and S.-H. Wei, *Physical Review B* **66**, 1 (2002).
  - <sup>10</sup> J. L. Lyons, a. Janotti, and C. G. Van de Walle, *Applied Physics Letters* **95**, 252105 (2009).
  - <sup>11</sup> G. Petretto and F. Bruneval, *Phys. Rev. Applied* **1**, 024005 (2014).
  - <sup>12</sup> S. Lany and A. Zunger, *Physical Review B - Condensed Matter and Materials Physics* **81**, 1 (2010).
  - <sup>13</sup> S. Sakong, J. Gutjahr, and P. Kratzer, *The Journal of chemical physics* **138**, 234702 (2013).
  - <sup>14</sup> M. C. Tarun, M. Z. Iqbal, and M. D. McCluskey, *AIP Advances* **1**, 0 (2011).
  - <sup>15</sup> M. D. McCluskey, C. D. Corolewski, J. Lv, M. C. Tarun, S. T. Teklemichael, E. D. Walter, M. Grant Norton, K. W. Harrison, and S. Ha, *Journal of Applied Physics* **117**, 112802 (2015).
  - <sup>16</sup> F. R. Petruzielo, J. Toulouse, and C. J. Umrigar, *Journal of Chemical Physics* **136**, 1 (2012), arXiv:1202.0317.
  - <sup>17</sup> W. Foulkes, L. Mitas, R. Needs, and G. Rajagopal, *Reviews of Modern Physics* **73**, 33 (2001).
  - <sup>18</sup> J. B. Anderson, *The Journal of Chemical Physics* **63**, 1499 (1975).
  - <sup>19</sup> J. W. Moskowitz, *The Journal of Chemical Physics* **77**, 349 (1982).
  - <sup>20</sup> P. J. Reynolds, *The Journal of Chemical Physics* **77**, 5593 (1982).
  - <sup>21</sup> E. Ertekin, V. Srinivasan, J. Ravichandran, P. B. Rossen, W. Siemons, A. Majumdar, R. Ramesh, and J. C. Grossman, *Physical Review B* **85**, 195460 (2012).
  - <sup>22</sup> J. a. Santana, J. T. Krogel, J. Kim, P. R. C. Kent, and F. a. Reboredo, *The Journal of Chemical Physics* **142**, 164705 (2015).
  - <sup>23</sup> J. A. Schiller, L. K. Wagner, and E. Ertekin, *Physical Review B - Condensed Matter and Materials Physics* **92**, 1 (2015), arXiv:1509.08321.
  - <sup>24</sup> J. Yu, L. K. Wagner, and E. Ertekin, *The Journal of Chemical Physics* **143**, 224707 (2015).
  - <sup>25</sup> N. D. Drummond, R. J. Needs, A. Sorouri, and W. M. C. Foulkes, *Physical Review B - Condensed Matter and Materials Physics* **78**, 1 (2008), arXiv:0806.0957.
  - <sup>26</sup> S. Chiesa, D. M. Ceperley, R. M. Martin, and M. Holzmann, *Physical Review Letters* **97**, 6 (2006).
  - <sup>27</sup> S. B. Zhang and J. E. Northrup, *Physical Review Letters* **67**, 2339 (1991).
  - <sup>28</sup> E. Burstein, *Phys. Rev.* **93**, 632 (1954).
  - <sup>29</sup> W. Carlos, E. Glaser, and D. Look, *Physica B: Condensed Matter* **308-310**, 976 (2001).
  - <sup>30</sup> L. K. Wagner, M. Bajdich, and L. Mitas, *Journal of Computational Physics* **228**, 3390 (2009).
  - <sup>31</sup> R. Dovesi, R. Orlando, A. Erba, C. M. Zicovich-Wilson, B. Civalleri, S. Casassa, L. Maschio, M. Ferrabone, M. De La Pierre, P. D'Arco, Y. Noël, M. Causà, M. Rérat, and B. Kirtman, *International Journal of Quantum Chemistry* **114**, 1287 (2014).
  - <sup>32</sup> J. R. Trail and R. J. Needs, *The Journal of chemical physics* **122**, 174109 (2005).
  - <sup>33</sup> J. R. Trail and R. J. Needs, *The Journal of chemical physics* **122**, 14112 (2005).
  - <sup>34</sup> M. Casula, *Physical Review B - Condensed Matter and Materials Physics* **74**, 1 (2006), arXiv:0610246 [cond-mat].
  - <sup>35</sup> As discussed in Refs. [12] and [13], larger supercells ( $> 198$  atoms) are needed to obtain a converged exchange splitting and orbital occupancy between the  $N\ 2p_{x,y}$  and  $2p_z$  levels. We caution that it is possible that this orbital ordering affects the trial wave functions used in our QMC simulation. In spite of this however, as noted previously<sup>13</sup>, DFT supercell total energies are converged to within 0.1 eV for 72 atom supercells.
  - <sup>36</sup> D. R. Burgess, in *NIST Chemistry WebBook, NIST Standard Reference Database Number 69*, edited by P. Linstrom and W. Mallard (National Institute of Standards and Technology, Gaithersburg, MD, retrieved 2016).
  - <sup>37</sup> Interestingly this estimate of the charged defect image interaction differs from our estimate in Section III.E, and was obtained using the Madelung term and the DFT-PBE estimate of the dielectric constant.
  - <sup>38</sup> J. Shim, E. K. Lee, Y. J. Lee, and R. M. Nieminen, *Physical Review B - Condensed Matter and Materials Physics* **71**, 1 (2005).
  - <sup>39</sup> N. D. M. Hine, K. Frensch, W. M. C. Foulkes, and M. W. Finnis, *Physical Review B - Condensed Matter and Materials Physics* **79**, 1 (2009).
  - <sup>40</sup> C. W. M. Castleton, a. Höglund, and S. Mirbt, *Physical Review B - Condensed Matter and Materials Physics* **73**, 1 (2006), arXiv:0512311 [cond-mat].
  - <sup>41</sup> M. Gerosa, C. Di Valentin, C. E. Bottani, G. Onida, and G. Pacchioni, *The Journal of Chemical Physics* **143**, 111103 (2015), <http://dx.doi.org/10.1063/1.4931405>.
  - <sup>42</sup> E. Ertekin, L. K. Wagner, and J. C. Grossman, *Physical Review B* **87**, 155210 (2013).